Proceedings Paper:
Sadraei, E, Romano, R orcid.org/0000-0002-2132-4077, Jamson, AH et al. (4 more authors) (2016) Understanding Cue Utility in Controlled Evasive Driving Manoeuvres: Optimizing Vestibular Cues for Simulator & Human Abilities. In: Sawaragi, T, (ed.) IFAC-PapersOnLine. The 13th IFAC/IFIP/IFORS/IEA Symposium on Analysis, Design, and Evaluation of Human-Machine Systems, 30 Aug - 02 Sep 2016, Kyoto, Japan. Elsevier , pp. 414-419.

https://doi.org/10.1016/j.ifacol.2016.10.601

Understanding Cue Utility in Controlled Evasive Driving Manoeuvres: Optimizing Vestibular Cues for Simulator & Human Abilities

E. Sadraei* R. Romano* S. Advani A.H. Jamson***
P. Chappell** G. Markkula* A. Bean**** E.R. Boer*,***

** Institute for Transport Studies, University of Leeds, UK, LS2 9JT*
(Tel: 744-270-6329; e-mail: {tsES, R.Romano, A.H.Jamson, G.Markkula @leeds.ac.uk}).
*** International Development of Technology, Breda, NL, (e-mail: s.advani@idt-engineering.com).*
**** Entropy Control, Inc., La Jolla, CA 92037 (Tel: +1-858-336-3571; e-mail: ErwinBoer@EntropyControl.com).*
*****, Jaguar Land Rover, 53G/17/2, Banbury Road, Gaydon, Warwick, CV35 0RR, UK*
(e-mail pchappel, abean@jaguarlandrover.com).

Abstract: Most daily driving tasks are of low bandwidth and therefore the relatively slow visual system receives enough cue information to perform the task in a manner that is statistically indistinguishable from reality. On the other hand, evasive maneuvers are of such a high bandwidth that waiting for the visual cues to change is too slow and skilled drivers use steering torques and vestibular motion cues to know how the car is responding in order to make rapid corrective actions. In this study we show for evasive maneuvers on snow and ice, for which we have real world data from skilled test drivers, that the choice of motion cuing algorithm (MCA) settings has a tremendous impact on the saliency of motion cues and their similarity with reality. We demonstrate this by introducing a novel optimization scheme to optimize the classic MCA in the context of an MCA-Simulator-Driver triplet of constraints. We incorporate the following four elements to tune the MCA for a particular maneuver: 1) acceleration profiles of the maneuver observed in reality, 2) vestibular motion perception model, 3) motion envelope constraints of the simulator, and 4) a set of heuristics extracted from the literature about human motion perception (i.e. coherence zones). Including these elements in the tuning process, notwithstanding the easiness of the tuning process, respects motion platform constraints and considers human perception. Moreover the inevitable phase and gain errors arising as a major consequence of MCA are always kept within the human coherence zones, and subsequently are not perceptible as false cues. It is expected that this approach to MCA tuning will increase the transfer of training from simulator to reality for evasive driving maneuvers where students need training most and are most dangerous to perform in reality.

Keywords: Driver maneuvers, motion cueing, optimization, coherence zone, simulator based training.

1. INTRODUCTION

1.1 Simulator Applications

Using a simulator as a virtual reality tool has diverse applications, such as training, research on driver/pilot behaviour, and the vehicle design procedure. Employing simulators has many advantages over the real world, it is cost effective and safer in hazardous conditions, and provides repeatable measurement and assessment on driver behaviour such as steering, pedal, engine profiles, vehicle motions, handling quality, etc. in diverse virtually prepared driving scenarios. It also provides easy control of variables such as traffic, weather, light timing, etc. during tests which cannot be experienced and measured repeatedly on road experiments (Carsten and Jamson, 2011). In other words, the availability, repeatability and controllability of driving variables with lower costs and risks has made simulators a vital tool for research and training and has motivated development of simulators in different configurations, sizes and cost.

In car manufacturing companies, advances in virtual vehicle design achieved through improved modelling accuracy of vehicle elements (e.g. vehicle dynamics) prior to prototype manufacturing has raised the application of driving simulators. Analytical design methods imply reduction of physical prototyping and the increased predictive capability of simulation tools. If this vision is to be realised, then the process of analytical design and verification needs to encompass not just the physical dimensions of component and system functionality, but also the perceptual experience from the driver's and passengers' perspective. One of the goals of the Programme for Simulation Innovation (PSi) is addressing how realistic simulators need to be to serve as a virtual prototyping tool, and what characteristics are necessary for it to be a reliable tool for virtual design evaluation. These questions are similar to those in training: what simulator characteristics are needed for it to serve as a viable alternative to real world training.

1.2 Simulator Motion Cuing Fidelity

While driving a vehicle on the road, a driver uses different visual, motion, aural and haptic cues to know absolute vehicle states as well as vehicle states relative to constraints in the environment. In other words, these cues affect driver

perception and shape the resulting driver behaviour (Hosman, 1996). Simulators try to replicate driving cues in a virtual environment. The similarity between these real world cues and their representation in simulators plus the informational value of these cues for the driving task at hand dictate the similarity between real world and simulator driving behaviour. Cue similarity is one measure of simulator fidelity. Many definitions of simulator fidelity are proposed (Heffley et al. (1981)). The fidelity of a training simulator is explained as a quality of the simulator that permits skilled pilots to perform a flying task in the same way that it is performed in the real aircraft. Apparently, among all cues, the visual and motion cues play more of a determinative role in the fidelity of simulators, especially in evasive manoeuvres with a disturbance.

This paper focuses on motion cuing and its limitations resulting in simulator fidelity reduction. Due to the fact that the vehicle motions are available to pilots/drivers in aircraft/car, intuitively motion cueing is necessary to be available in simulators to have a training effect similar to real world training. It is proved by many authors that motion cuing is absolutely necessary to achieve acceptable training transfer of aircraft control in simulators (Mulder et al., 2004).

1.3 Simulator Components and Limitations

The discrepancy between driving simulators and the real world in terms of representing the motion cues originates from three main components in simulators that have an impact on motion cuing: the vehicle model, motion cueing algorithm (MCA) and the simulator's motion platform (MP). The vehicle model is generating the vehicle motion outputs (displacements, velocity and accelerations) with respect to the driver control input (steering, throttle, brake). In the ideal case the vehicle accelerations should be replicated identically by the MP, but due to the limited physical capabilities of an MP not all of the desired motions can be rendered one to one. The MCA is mainly designed to take care of the MP's limitation i.e. representing the vehicle motions while keeping them within the MP's motion envelope. As a result, the vehicle motions pass through the MCA and then to the MP. Both the MCA and MP are added to the dynamics of the controlled system (vehicle model) and the driver perceives the controlled system as the combination of these three.

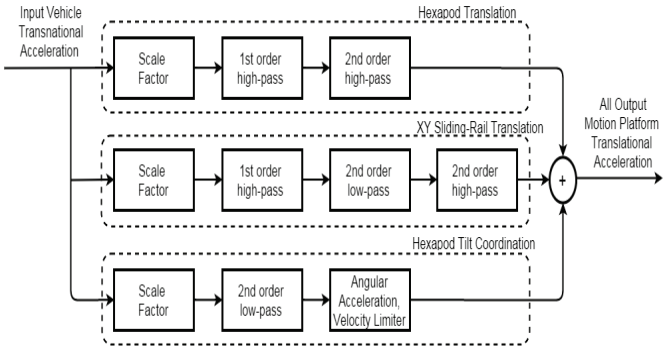

Fig. 1. Classic MCA used in this study

The most commonly used MCA in simulators is a classical algorithm which is a combination of scale factors, high and low pass filters and limiters as its main components. The classic MCA was first introduced by (Conrad and Schmidt, 1970) for flight simulator as a solution for to compromise between one to one acceleration rendering and motion system constraints. A comprehensive description about its concept and function is provided by Grant and Reid, (1997). Various combinations of filters with different orders have been employed in literature which are selected depending on the end value theorem of filter responses and presence or absence of washout behaviour in them (Reid and Nahon, 1985). This study uses the one shown in Fig. 1.

The selection of parameters for the digital filters in MCA is called tuning the algorithm which is a trade-off between maximizing cue reproduction while eliminating motion commands that are outside the envelope and capability constraints of the MP. The classical MCA is usually tuned before the start of the simulation for the worst-case scenario so that the MP does not exceed its envelope and performance capability while representing the maximum portion of vehicle motions to participants. Consequently, there is an inevitable discrepancy that MCA adds in motion cueing in simulators, which can be captured in time domain motion cuing amplitude error or in the frequency domain's phase and gain error between the vehicle motion output and MP's motion output (Romano, 2003).

1.4 Motion Perception and Coherence Zones

Motion perception about position and velocity is mainly received through the visual system, while perception about acceleration is received through the vestibular system. It provides information for the sense of balance and spatial orientation of the body to support movement. The vestibular system consists of a semi-circular canal (SCC) and Otolith that are sensors of rotational and translational accelerations respectively. There has been much prior research into addressing the characteristics, thresholds and modeling of the Otolith and SCC. This paper will use the Otolith model which is employed by Telban and Cardullo (2005) in developing their cuing algorithm which is described in (1). The $\hat{f}$ is the sensed specific force which is related to stimulus specific force f, the input to Otolith model. A 0.4 gain takes care of the acceleration perception threshold.

$$\frac{\hat{f}}{f} = 0.4\frac{(10s+1)}{(5s+1)(0.016s+1)} \tag{1}$$

However, in driving, the motion cue is never alone and it is always coupled with visual cues. It has been the subject of study for many years to address the maximum undetectable phase and amplitude distortion (coherence zones) between the visual and motion cues in flight simulators, to find out how this discrepancy between visual and motion cues affect the driver sensation, perception, control performance and behaviour in simulators. The amplitude coherence zone refers to the range of motion cue magnitude attenuation that,

although not being a perfect match to the visual cue is still perceived by drivers to be coherent. A similar definition exists for phase coherence zone. It is shown that coherence zones are both functions of visual cue amplitude and frequency (Valente Pais, 2013). Much more research is needed however to understand the effect of active control on these coherence zones as well as the effect of natural perturbations.

An example for the amplitude coherence zone for the sway motions is represented in Fig. 2. It shows the amplitude coherence zones as coloured bars for two visual acceleration amplitudes of 0.1 and 1 m/s^2 in three frequencies of 2, 3, 5 rad/s on horizontal axis, and motion gain on vertical axis. The range of bars shows the zones. The trends in the data shows that both the upper and lower threshold gains decrease slightly with increasing frequency and the gains are lower for the highest amplitude of the visual cue (i.e. the coherence zone is narrower for stronger visual signals).

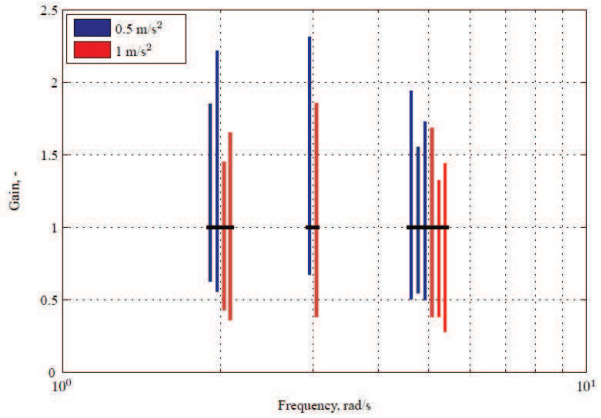

Fig. 2. Coherence zones represented as the maximum and minimum motion gains obtained from the threshold values, across all amplitudes and all sway motion, reproduced from (Valente Pais, 2013).

Knowledge of motion perception coherence zones helps to find the best MCA tuning settings for a motion platform because it provides more freedom to address the motion platform minimum requirement. This paper focuses on the classical MCA and tuning its parameters through a mathematical optimization approach that considers both limitations of the motion platform as well as the coherence zones. The parameter tuning is undertaken for a near limit slalom manoeuvre. The whole parameter optimization procedure is novel because it includes temporal matching to target accelerations, MP constraints and coherence zones. Section two describes the methodology for optimization which is followed by the presentation of results and in section three there is a discussion and conclusion.

2. METHODOLOGY AND RESULTS

2.1 Tuning Approaches

The MCA parameter tuning is a mathematical process among the driving tasks, vehicle dynamic, MCA and MP to come up with a set of parameters that minimizes the motion cuing errors between virtual and real world, while also taking into account human perception and behaviour. Considering driver behaviour to find the parameters is a closed-loop approach. It means in a driving task the driver senses the feedback of the motion cues in the simulator to actively perceive the cues and gains an understanding about current and future vehicle states, and then performs an action to control the vehicle. Conversely, tuning for passive human perception is considered as open-loop because no active driver control is required and the driver sits in the simulator without controlling the vehicle.

Trial and error can be used to take the driver/pilot perception into account for finding the MCA parameters. Different parameter settings can be implemented in the simulator and the drivers asked about their perception about the different settings to draw a conclusion. This needs a lot of effort and in the end may not get to a solid conclusion about realistic settings. Alternatively, the candidate settings can be found through offline analysis. This needs to have all the real world elements of the human and simulator modelled and integrated in an offline open-loop (i.e. for now without a driver model that can predict the effect of different MCA settings on control behaviour) analysis environment, incorporating models of human perception, vehicle characteristics, MCA, motion platform, and coherence zone thresholds. Accurate models of all components are available in the literature to allow offline tuning.

2.2 Optimization Process

As can be seen in Fig. 4 all the models are prepared a priori and integrated in an offline optimization environment in Matlab/Simulink. Vehicle motions are the real vehicle motions measured from an instrumented Jaguar S-Type car driven on ice-lake test tracks in Sweden with low friction conditions by Jaguar Land Rover professional drivers. The vehicle acceleration profiles are measured both by an inertial measurement unit (IMU) and GPS data. Figure 3 shows the acceleration profiles for the slalom task for different drivers.

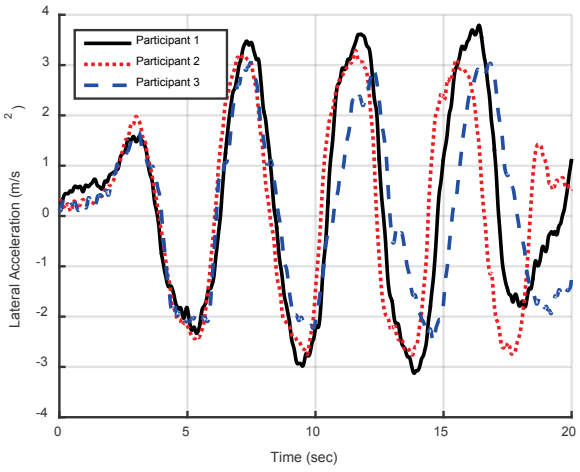

Fig. 3. Lateral acceleration profiles of three participants in Slalom task

The classic MCA as described in the previous section is employed in the optimization. It is tuned for the lateral translational channel that incorporates the hexapod and sliding rail and avoids activating the tilt-coordination in the optimal tuning process. The reason for this is to use the MP as much as possible without relying on tilting to represent the motions to the driver, as well as the fact that the 5m wide sliding rail of the MP is capable of handling the tasks in sway direction acceptably without the need for tilting (Jamson, 2010). The parameters of the MCA are the cut-off frequencies of the filters which are shown in Fig. 1, by w_hp1_hex which means cut-off frequency of first high pass filter of hexapod, and the scale factors, these are in fact the input variables of optimization shown in Fig. 4, and the damping ratio for all filters have the same value of 1. Allowing this parameter in the optimization would add more complexity to the optimization, but may improve results. The comparison between target acceleration profiles and MCA produced acceleration profiles is performed after these profiles are passed through the vestibular model to assure that the comparison is performed based on what humans can actually perceive. The red arrows in Fig. 4 indicate that the frequency range of the manoeuvre is used to place extra emphasis on assuring that those frequencies are reproduced well. For the frequency based constraints a bode plot of the MCA plus MP plus Vestibular System is generated each iteration.

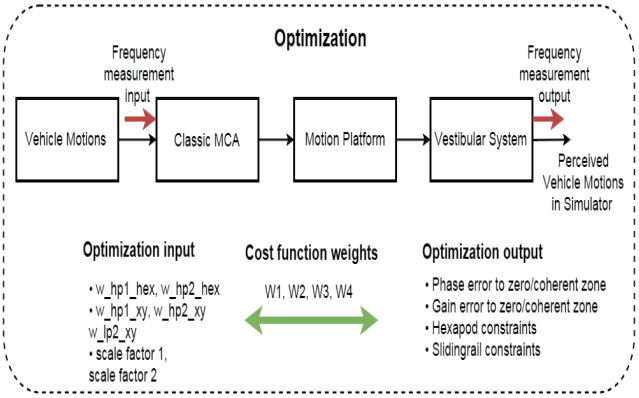

Fig 4. Optimization Process.

The motion platform model of the University of Leeds driving simulator (Jamson, 2010) is developed from measured inertial measurement unit (IMU) responses of the platform in each single degree of freedom independently. They are modelled as transfer functions that were generated from the data. The motion platform's hexapod also has a cross-coupling which means that excursions in one direction limit the motion envelope available another direction. However the MCA is being tuned only in its single lateral acceleration channel so that the MP's model reflects the real MP's performance. The MP's motion envelope constraints are also considered in the optimization to find the MCA parameters. The otolith model was introduced earlier and shown in (1).

The optimization cost function is a combination of goals and constraints. The constraints detailed below need to be satisfied and once they are the goal should be met as well as possible. If the constraints cannot be satisfied by the optimization, then the constraints need to be relaxed until they can be met. The only goal is the squared error between an observed real world slalom acceleration profile and the accelerations produced by the MCA. Two types of constraints are incorporated. The first is that the position of the hexapod and the sliding rail do not exceed their hard lateral motion limits ($\pm 2.5m$ for rail and $\pm 0.318m$ for the hexapod). The second is a set of gain and phase tolerance ranges around the optimal gain of 0dB (unity) and the optimal phase of zero degrees. These gain and phase tolerances can be used to encode the coherence zones (more research is needed to produce those for driving manoeuvres). Here we provide a proof of concept demonstration that the optimization is capable of tuning the free MCA parameters such that imposed phase and gain tolerances are satisfied. The green lines in Fig. 5 depict a 5dB gain tolerance and a 30 degree phase tolerance between 0.16Hz and 10Hz in the bode plots. Note that this frequency range should ideally span the frequencies that occur in the real world manoeuvre (as they do for the slalom here). Outside this frequency range the gain tolerance is 100dB and the phase tolerance 300 degrees.

All the information in Fig. 2 is for sway in a passive task and it is available for only a few frequencies and amplitudes of the visual stimuli. As can be seen from Fig. 3 the frequency of the slalom driving task is around 0.2 Hz or 1.26 rad/sec and the amplitude 4 m/s^2. These are the visual frequencies and amplitudes to use for extracting the coherence upper and lower boundaries from Fig. 2 and as can be seen the corresponding data in not available in the figure. Therefore data collection is required for the phase and amplitude coherence zones in the slalom manoeuvre's amplitude and frequency. This will be subject of future research.

To incorporate coherence zones into the optimization, a unique cost function is developed by including the optimization goals as described in (2). The first line of the cost function carries the responsibility of minimizing the temporal difference between the target real world acceleration (slalom here) and the accelerations of the motion platform. The superscript p indicates that these accelerations are compared after passing through the vestibular model. A weight w_0 is assigned to the acceleration error. The next line forces the gain error in dB to zero and the phase error in degree to zero. The frequency range over which this is performed should match the frequency range observed in the manoeuvre. Below we provide an alternative solution to gain and phase fitting. The final two lines take care of hexapod and sliding rail position envelope constraints using exponential functions. The functions work in a way that when the MB is getting closer to the boundaries the exponential functions increase the values in the cost function and results in a change of input parameters to avoid hitting boundaries. There are also different weights available separately for hexapod and sliding rail i.e. w3 and w4 which shows how steep the exponential functions would behave near the boundary. By increasing the w3 and w4 weights the response

of the exponential function gets steeper. Practically these exponential weights can be large as long as they do not cause numerical overflow errors.

$$\sum_{t=t_1}^{t_2}\left\{w_0\left(a_{slalom}^{p}-a_{mp}^{p}\right)_t^2\right\}+$$
$$\sum_{f=f_{\min}}^{f_{\max}}\left\{w_1*GainError_f^2+w_2*PhaseError_f^2\right\}+ \quad (2)$$
$$\sum_{t=t_1}^{t_2}\left\{\begin{matrix}\exp^{(w3*(PosHexNow-PosHexMax))}+\exp^{(-w3*(PosHexNow-PosHexMin))}+\\ \exp^{(w4*(PosXYNow-PosXYMax))}+\exp^{(-w4*(PosXYNow-PosXYMin))}\end{matrix}\right\}$$

Given that the MCA is a combination of filters that together should produce a transfer function with unity gain (0dB) and zero phase because then reality is veridically replicated. However, a completely flat response over a wide frequency range is practically impossible. It is therefore important to focus on the frequencies in the target manoeuvre as well as the human tolerances in noticing phase and gain error.

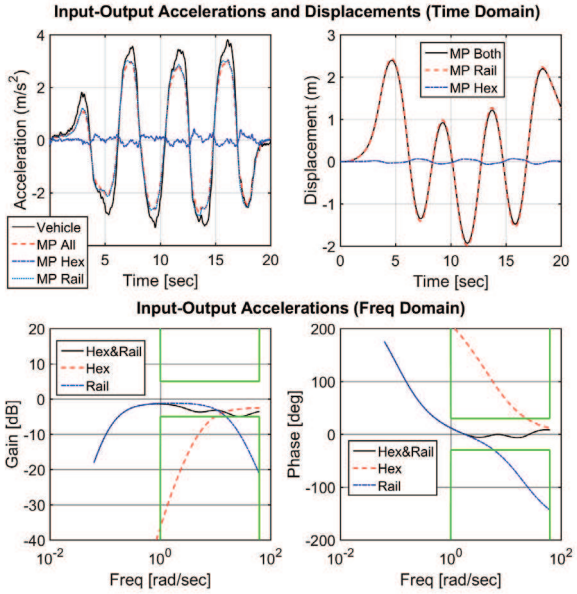

Fig. 5. Result of MCA filter and scale factor tuning using time and frequency constrained optimization for a low friction slalom manoeuvre. The green lines indicate the hypothetical gain and phase coherence tolerances across frequencies present in a slalom manoeuvre.

In the previous cost function (2) the weights w_1 and w_2 need to be selected which is less than trivial. Since we can capture the coherence zones in terms of gain and phase tolerances (again research is needed to establish this for driving), the 2nd line in cost function (2) can be replaced by (3).

$$\sum_{f=f_{\min}}^{f_{\max}}\left\{\begin{matrix}\exp^{w1*(GainNow_f-GainMaxCoh_f)}+\exp^{-w1*(GainNow_f-GainMinCoh_f)}+\\ \exp^{w2*(PhaseNow_f-PhaseMaxCoh_f)}+\exp^{-w2*(PhaseNow_f-PhaseMinCoh_f)}\end{matrix}\right\} \quad (3)$$

The maximum and minimum gain and phase tolerances that assure coherence between visual and vestibular perception of the vehicle motion, can take on complex forms; here we adopt for sake of demonstration the forms show in green in the bottom two panels of Fig. 5.

The optimization was run for the slalom manoeuvre in Fig. 3; the results of which are presented in Fig. 5 and 6 as well as Table 1. The top panels in Fig. 5 show accelerations and displacements of the real vehicle, the MP's hexapod, sliding rail and both together are shown in time domain. In the bottom panels the frequency response of the integrated model between the red arrows in Fig. 4 are shown. It is clear that the optimization was able to adjust the filter parameters and scale factors such that the gain and phase constraints were met. In other words, the transfer function of MCA+MP passed through the vestibular model is sufficiently flat (i.e. according to assumed coherence gain and phase tolerances) within the frequency range relevant for the target slalom manoeuvre. From Fig. 6 it is clear that the position constraints on the rail and hexapod were also satisfied.

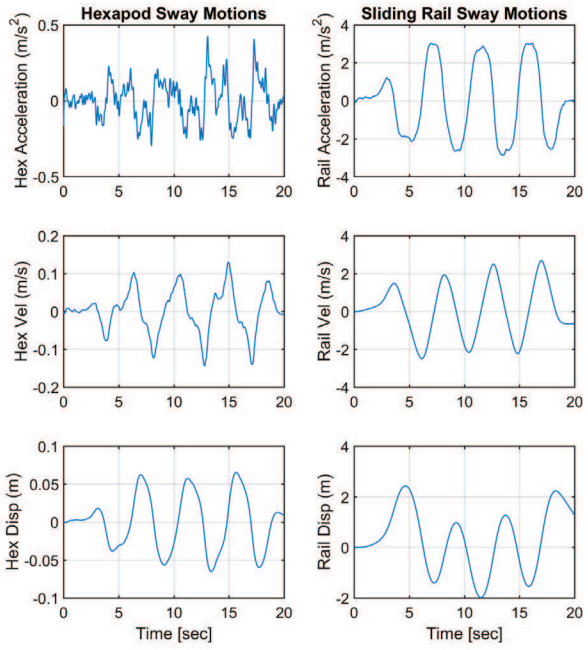

Fig. 6. Hexapod and sliding rail position, velocity and acceleration profiles generated for the target slalom manoeuvre; see text and Fig 5 caption for more details.

The filter coefficients and scale factors resulting from the optimization are detailed in Table. 1. It is important to note that the scale factors were free parameters in the optimization and that their final values are not unity. The reason is that for the chosen frequency range (green constraints in Fig. 5), in order to reproduce the lowest frequency with a gain that deviates no more than 5dB from the optimal 0dB and a phase that deviates no more than 30 degrees from the optimal zero, it was only possible to do so with a scale factor of 0.88 on the rail without violating its excursion constraints. If the lowest frequency in the green coherence profile is increased, unity

scale factors can be achieved which means only over the "green" frequency range.

Table 1. Optimization parameter results for slalom.

Sliding Rail Filters		Hexapod Filters	
Cut-off frequency (rad/sec)			
ω_hp1_xy	0.1110	ω_hp1_hex	1.1382
ω_hp2_xy	0.0994	ω_hp2_hex	5.6813
ω_lp1_xy	20.6424		
Scale factor			
Scale factor	0.8814	Scale factor	0.7525

The adopted approach gives more freedom to the optimization process to choose the parameter settings that satisfy the phase and gain thresholds because within these phase and gain tolerance the optimization can shift cut-off frequencies around and manipulate scale factors such that an acceptable ripple in the overall transfer function is achieved (akin to digital filter design).

3. DISCUSSION AND CONCLUSIONS

A novel optimization scheme for tuning classical MCA was developed to overcome the main difficulties accompanying current MCA tuning process, such as needing a lot of trial and error to find a solution that satisfies all constraints. The introduced tuning scheme integrates task (acceleration time series), motion platform (excursion constraints) and human perception (gain and phase tolerances in motion rendering transfer function). The optimization has no cost function terms to trade off because it has no weights to select. The weights on the exponential constraint terms should be high (we used 500) so that once the constraints are satisfied, these terms do no longer impact the overall cost within the satisficing domain. Within this satisficing domain, the only operating cost term is error between observed and generated acceleration profiles and thus any weight results in the same minimum point.

The method must be further extended to cover many other issues, such as including the tilt coordination channel and variable damping ratio into the optimization. Also all of the motion channels need to be tuned at the same time to take into account the limitation of simultaneous excursions of the motion platform. Moreover, to include the coherence zones into the analysis, data needs to be collected experimentally for different driving tasks in at least the surge, sway and yaw channels, because the available data in literature are limited to a few flying manoeuvres. We expect that by collecting the coherence zone data and including it in optimization and finding the filter parameters MCA parameters can be automatically obtained that yield high quality motion rendering. To confirm these expectations, a series of experiments will be conducted in the University of Leeds Driving Simulator (Jamson 2010).

As a cautionary note, it is good to recognize that using this tuning method with coherence zones does not guaranty the simulator to be of high fidelity because the MP may not have enough capability to reproduce the motion without false cues. However we can be sure that in employing the classical MCA for a MP we cannot get any higher motion cuing fidelity (gain and phase errors within coherence zone). Future research could extend the algorithm to also address the necessary MP size and capability to be suitable for virtual training and prototyping. Within the EPSRC/JLR Programme for Simulation and Innovation we aim to put task specific numbers on otherwise nebulous terms such as fidelity.

ACKNOWLEDGMENTS

This work was supported by Jaguar Land Rover and the UK-EPSRC grant EP/K014145/1 as part of the jointly funded Programme for Simulation Innovation.

REFERENCES

Carsten, O. & Jamson, A. H. 2011. Driving simulators as research tools in traffic psychology. *Handbook of traffic psychology*, 87-96.

Conrad, B. & Schmidt, S. 1970. Motion drive signals for piloted flight simulators.

Grant, P. R. & Reid, L. D. 1997. Motion Washout Filter Tuning: Rules and Requirements. *Journal of Aircraft,* 34, 145-151.

Heffley, R. K., Clement, W. F., Ringland, R. F., Jewell, W. F. & Jex, H. R. 1981. Determination of Motion and Visual System Requirements for Flight Training Simulators. DTIC Document.

Hosman, R. 1996. *Pilot's perception in the control of aircraft motions.* PhD, Delft University of Technology.

Jamson, A.H.J. (2010) Motion cueing in driving simulators for research applications. PhD thesis, Univ. of Leeds.

Mulder, M., Paassen, M. & Boer, E. 2004. Exploring the Roles of Information in the Manual Control of Vehicular Locomotion: From Kinematics and Dynamics to Cybernetics. *Presence,* 13, 535-548.

Reid, L. D. & Nahon, M. A. 1985. Flight Simulation Motion-Base Drive Algorithms: Part 1 - Developing and Testing the Equations. University of Toronto: Institute for Aerospace Studies

Romano, R. Non-linear optimal tilt coordination for washout algorithms. AIAA Modeling and Simulation Technologies Conference and Exhibit, 2003.

Telban, R. J. & Cardullo, F. M. 2005. Motion cueing algorithm development: Human-centered linear and nonlinear approaches.

Valente Pais, A. 2013. *Perception Coherence Zones in Vehicle Simulation.* PhD, Delft University of Technology.